

Physical Response of Geomembrane Wrinkles Overlying Compacted Clay

S. Gudina¹ and R. W. I. Brachman²

Abstract: The short-term physical response of a 1.5-mm-thick, high-density polyethylene geomembrane with an artificially formed wrinkle and overlying three different subgrade materials (sand and compacted clay at two initial water contents) are reported. The influence of the subgrade, protection layer, backfill, and applied pressure on the fate of the gap beneath the wrinkle, wrinkle deformations, and local geomembrane indentations is investigated. The gap beneath the geomembrane wrinkle was observed to remain with sand above and below the geomembrane, even at applied pressures of 1,100 kPa. The gap was eliminated with compacted clay as the subgrade, depending on the applied pressure and the clay water content. When the clay was compacted at a water content equal to the standard Proctor optimum (ω_{opt})+4%, the gap was eliminated at pressures greater than 100 kPa, whereas the gap remained at 250 kPa and was eliminated at 500 kPa and larger when compacted at ω_{opt} +1%. It was found that the presence of a wrinkle increases the maximum geomembrane strain due to local gravel indentations by 10% as compared to a flat geomembrane. The protection layers tested did not significantly influence the change in height and width of the wrinkle, but did influence the local geomembrane strain. The maximum strain in the geomembrane (at 250 kPa with 50 mm gravel backfill and the softer clay subgrade) was 42% without protection; 15 and 11% with nonwoven needle-punched geotextiles with mass per unit area of 390 and 1,200 g/m², respectively; and 2% with a 150-mm-thick sand protection layer.

DOI: 10.1061/(ASCE)1090-0241(2006)132:10(1346)

CE Database subject headings: Geomembranes; Clays; Lining; Landfills.

Introduction

Composite liners consisting of a geomembrane (GM) overlying compacted clay (CCL) are an important component of barrier systems that provide environmental protection in modern waste containment facilities. The primary function of the geomembrane is to impede the advective flow of contaminants through the liner (limited to leakage through holes in the GM) and to provide a diffusive barrier to inorganic contaminants (e.g., Rowe et al. 2004). During installation of the liner, material expansion caused by solar heating and/or placement of overlying materials may lead to wrinkles in the geomembrane. As shown in Fig. 1, a wrinkle prevents contact between the geomembrane and the underlying material as a physical gap initially exists beneath the wrinkle.

The wrinkle may lead to increased leakage through a hole in the geomembrane at or near the wrinkle, because the geomembrane is not in direct contact with the underlying material. Solutions are available to quantify the potential leakage through a hole

in a wrinkle (Rowe et al. 2004). The extent to which the gap beneath the wrinkle may decrease when buried is of interest. There is also increased potential for stress cracking due to the tensile strains that are induced by the wrinkle when subject to vertical pressures (from the weight of the overlying waste), and these may be compounded by other local tensile strains arising from coarse gravel backfill above the geomembrane (see Fig. 1). The magnitudes of deformation and strain in the wrinkle have been reported for the specific case with sand above and below the geomembrane wrinkle (Soong and Koerner 1998). Their results showed that, although the wrinkle experienced a decrease in height and width, the gap beneath the wrinkle remained even when subjected to a pressure of up to 1,100 kPa and a test duration of 1,000 h. The magnitude of short-term tensile strains in the geomembrane arising from coarse gravel backfill have been reported by Tognon et al. (2000) for a composite GM/CCL, but without a wrinkle. However, it is uncertain whether the wrinkle itself alters these local strains because of redistribution of vertical stresses around the wrinkle.

The objective of this paper is to present results from short-term experiments to quantify the physical response of geomembrane wrinkles when overlying a compacted clay liner and with a coarse gravel backfill. The influence of the type of subgrade, backfill, and protection layer on the fate of the gap beneath the wrinkle, wrinkle deformations, and local geomembrane indentations is examined.

Experimental Details

Test Cell and Boundary Conditions

A cross section through the test cell with an inside diameter of 590 mm and a height of 500 mm is shown in Fig. 1. Vertical

¹Graduate Student, GeoEngineering Centre at Queen's-RMC, Queen's Univ., Kingston ON, Canada, K7L 3N6. E-mail: simon@civil.queensu.ca

²Associate Professor, GeoEngineering Centre at Queen's-RMC, Queen's Univ., Kingston ON, Canada, K7L 3N6 (corresponding author). E-mail: brachman@civil.queensu.ca

Note. Discussion open until March 1, 2007. Separate discussions must be submitted for individual papers. To extend the closing date by one month, a written request must be filed with the ASCE Managing Editor. The manuscript for this paper was submitted for review and possible publication on December 1, 2005; approved on April 2, 2006. This paper is part of the *Journal of Geotechnical and Geoenvironmental Engineering*, Vol. 132, No. 10, October 1, 2006. ©ASCE, ISSN 1090-0241/2006/10-1346-1353/\$25.00.

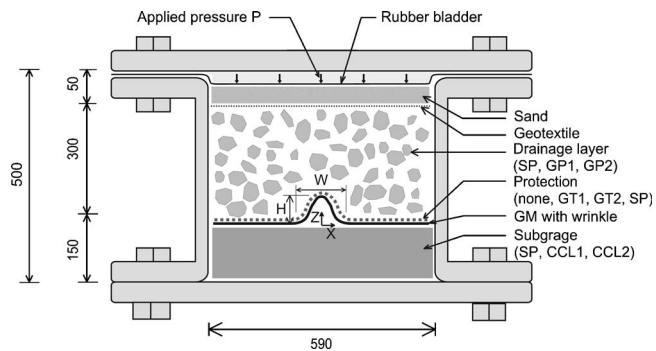


Fig. 1. Cross section through test cell showing geomembrane wrinkle and configurations tested (all dimensions in mm)

pressures are applied by a rubber bladder inflated with fluid pressure. Horizontal stresses corresponding to zero lateral strain conditions develop by limiting outward deflection of the test cell. Because only a finite size of the geomembrane wrinkle and surrounding soil materials can be tested in the laboratory, careful selection of the dimensions of the test cell and assessment of the boundary roughness were required to minimize boundary effects. To reduce boundary friction, the vertical boundaries of the test cell were covered with two 0.1-mm-thick polyethylene sheets lubricated with grease (DOW Corning 44) to allow slip between the sheets. Tognon et al. (1999) showed that this arrangement reduces boundary friction to less than 5° . For its size and with the friction treatment, 95% of the applied vertical pressure is calculated to act at the elevation of the geomembrane (Brachman and Gudina 2002). Because the effect of boundary friction is minimized, but not eliminated, the reported values of applied pressure should be reduced by 5% when considering an equivalent burial pressure in a landfill.

Two choices were made regarding the boundary conditions of the geomembrane. First, the end boundary condition of the geomembrane in the transverse (X) direction was designed to provide zero displacement in the X -direction without restraining the vertical (Z) displacement. Second, it was chosen to provide zero axial (Y) restraint where the ends of the wrinkle met the test cell wall (at $|Y| = 295$ mm). This was achieved by leaving a 5 mm gap between the test cell wall at each end of the geomembrane wrinkle, thus preventing the geomembrane from binding against the wall. Three-dimensional finite-element analysis (Brachman and Gudina 2002) has shown that this boundary condition results in negligible effects ($<0.1\%$ difference in vertical deflection) relative to axial plane strain conditions (those expected to prevail for a long wrinkle in the field) for the central 120 mm of the test specimen, for which all results were reported.

Materials and Test Procedure

A summary of the materials and configurations tested is given in Table 1. A temperature of 22°C was maintained for all tests. Three different subgrades were tested. Poorly graded sand (SP) was used as a reference case and to provide a comparison with the data of Soong and Koerner (1998). The sand subgrade was compacted to achieve a dry density of 1.75 g/cm^3 at a water content of 0.2%. Tests were also conducted with a compacted clay liner beneath the geomembrane. The silty clay (CL) tested was obtained from a landfill site in Milton, Ontario, Canada, and had a liquid limit of 26%, a plastic limit of 16%, and a grain size with 32% finer by mass than $2\ \mu\text{m}$. For standard Proctor compaction,

the clay had a maximum dry density of 2.1 g/cm^3 at an optimum water content, ω_{opt} of 12%. Tests were conducted at molding water contents of approximately 16% (denoted as CCL1) and 13% (denoted CCL2) to investigate the effect of clay subgrade stiffness on the wrinkle. The clay was compacted in three 50-mm-thick lifts. In-place dry densities of 1.9 and 2.0 g/cm^3 were achieved for CCL1 and CCL2, respectively.

The geomembrane was placed after the subgrade was leveled. A 1.5-mm-thick high-density polyethylene (HDPE) geomembrane that meets GRI-GM13 (Geosynthetic Institute 2003) was tested. The stress-strain properties of the particular geomembrane tested are reported in Table 2. They were obtained in accordance with ASTM D 5323 and D 6693 (ASTM 1992, 2001) on five samples each in the machine and cross-machine directions. It should be recognized that not all HDPE geomembranes have the same properties; consequently, care is required if the results in this paper are applied to another 1.5-mm-thick HDPE geomembrane. At present, it may be best to test the specific materials (backfill, protection layer, geomembrane, and subgrade) to obtain the results for a particular project.

A wrinkle was manually formed in the geomembrane. All tests except Test 15 were conducted with an initial wrinkle height of $H_0 = 60$ mm and wrinkle width $W_0 = 240$ mm. Test 15 was conducted with $H_0 = 30$ mm and $W_0 = 200$ mm to examine a smaller wrinkle. These wrinkle sizes are within the range of field observations reported by Pelte et al. (1994) for a 1.5-mm-thick black HDPE geomembrane overlying clay in a 30×30 m landfill cell. The initial geometry of the wrinkle was measured to an accuracy of ± 0.1 mm using a profiler consisting of a series of displacement transducers attached to a linear rail.

Three different granular materials (denoted as GP1, GP2, and SP) were tested to simulate the drainage layer overlying the geomembrane. Grain size distribution curves are given in Fig. 2. The nominal 50 mm gravel (GP1) meets the requirements of Ontario, Canada landfill regulations [Ontario Ministry of the Environment (MOE) 1998], while the nominal 25 mm gravel (GP2) satisfies German regulations [Bundesanstalt für Materialforschung und-Prüfung (BAM) 1995]. The SP and GP materials were placed in a relatively loose condition with respective bulk densities of approximately 1.72 and 1.50 g/cm^3 . After the desired backfill height of 300 mm was reached, a 50-mm-thick leveling sand layer (fine to medium sand) was placed above the granular backfill to prevent damage to the rubber bladder. A geotextile was used to separate the drainage layer and the leveling sand.

Although some sort of protection layer would most certainly be used in the field when using gravel above the geomembrane, Tests 3–7 were conducted without protection to serve as a reference. For Tests 8–15, the geomembrane was covered with a protection layer. Two nonwoven needle-punched geotextiles (GT1 and GT2 with masses per unit area equal to 390 and $1,200\text{ g/m}^2$, respectively) and a 150-mm-thick layer of poorly graded sand (SP) were tested.

Vertical pressures were applied in increments every 10 min, using 50 kPa increments for most tests and 100 kPa increments for tests to 1,000 kPa, and then were held constant for 10 h (with the exception of Test 7, as discussed later). The airspace of the gap beneath the geomembrane was maintained at atmospheric pressure. At the end of each test, but while the pressure was still being applied, a low-shrinkage grout made from plaster of Paris was injected into any remaining gap(s) beneath the geomembrane to preserve the final geometry. After curing of the grout, the backfill material was removed and the final geometry of the wrinkle was measured using the profiler to an accuracy of ± 0.1 mm.

Table 1. Summary of Test Configurations and Results, Initial Wrinkle Height $H_0=60$ mm and Width $W_0=240$ mm, Except for Test 15, Where $H_0=30$ mm and $W_0=200$ mm

Test	Test configuration			ω_{CCL} (%)	Pressure (kPa)	Final wrinkle geometry		
	Backfill	Protection layer	Subgrade			H (mm)	W (mm)	$\kappa \times 10^{-2}$ (-)
1a	SP	None	SP	-	250	32.4	95	5.4
1b	SP	None	SP	-	250	30.0	85	4.7
2a	SP	None	SP	-	1,100	30.5	75	7.2
2b	SP	None	SP	-	1,100	29.2	65	11
3	GP1	None	CCL1	16.0	50	53.0	220	2.9
4	GP1	None	CCL1	15.6	100	40.0	190	1.8
5a	GP1	None	CCL1	16.1	250	35.7	200	2.4
5b	GP1	None	CCL1	15.8	250	42.9	196	2.4
5c	GP1	None	CCL1	15.4	250	42.9	193	2.5
6a	GP1	None	CCL1	15.9	1,000	43.2	190	3.2
6b	GP1	None	CCL1	16.0	1,000	37.5	195	2.3
7	GP1	None	CCL1	16.5	250	47.0	185	2.4
8a	GP1	GT1	CCL1	16.1	250	44.6	191	3.3
8b	GP1	GT1	CCL1	16.0	250	52.9	207	1.6
8c	GP1	GT1	CCL1	16.0	250	50.0	189	2.0
9a	GP1	GT2	CCL1	15.6	250	40.0	193	2.3
9b	GP1	GT2	CCL1	16.0	250	42.9	207	3.0
9c	GP1	GT2	CCL1	15.5	250	42.9	211	2.1
10	GP1	SP	CCL1	16.6	250	51	190	3.2
11	GP1	GT2	CCL2	12.9	250	31	175	9.2
12	GP1	GT2	CCL2	13.0	500	36	180	9.1
13	GP1	GT2	CCL2	12.7	1,000	30	205	21
14a	GP2	GT2	CCL1	16.5	250	43.0	210	2.2
14b	GP2	GT2	CCL1	16.1	250	44.0	215	2.2
14c	GP2	GT2	CCL1	16.6	250	50.0	195	2.9
15a	GP1	GT2	CCL1	15.4	250	18.0	155	1.8
15b	GP1	GT2	CCL1	15.7	250	20.0	170	1.1
15c	GP1	GT2	CCL1	16.1	250	15.0	160	1.1

Results

Sand Above and Below Geomembrane Wrinkle

Results obtained with sand above and below the geomembrane are examined first, prior to the more complex conditions with gravel and clay. Fig. 3 shows the initial and deformed shapes of the geomembrane from two tests conducted to 250 kPa. The initial and final wrinkle shapes were very similar between the two duplicate tests, and the average of these two tests (Tests 1a and b) is plotted in Fig. 3(a). The plot shows that the wrinkle height and width were reduced to 52% (31 mm) and 37% (90 mm) of their original values. Fig. 3(b) shows a cross section along the Y -axis.

Table 2. Stress-Strain Properties (Mean \pm 95% Confidence Interval) of Particular Geomembrane Tested, Obtained Following ASTM D 5323 and D 6693 (ASTM 1992, 2001)

Property	Machine direction	Cross-machine direction
Yield strength (kN/m)	30 \pm 0.6	31 \pm 0.6
Break yield strength (kN/m)	49 \pm 4	53 \pm 5
Yield elongation strain (%)	21 \pm 0.4	19 \pm 0.5
Break elongation strain (%)	770 \pm 70	880 \pm 80
2% secant modulus (MPa)	310 \pm 10	320 \pm 26

There was little variation in the wrinkle deformation along the Y -axis, with a coefficient of variation of less than 3%. The consistent deflection along the wrinkle was expected with the continuous loading provided by the sand backfill. The results in Fig. 3(b) show no discernible effect from the end boundaries on wrinkle deformation.

The final shape of the geomembrane wrinkle when subjected to a vertical pressure of 1,100 kPa for otherwise the same test conditions as in Test 1 is also plotted in Fig. 3 (Test 2). These results are also the average of two duplicate tests (Tests 2a and b),

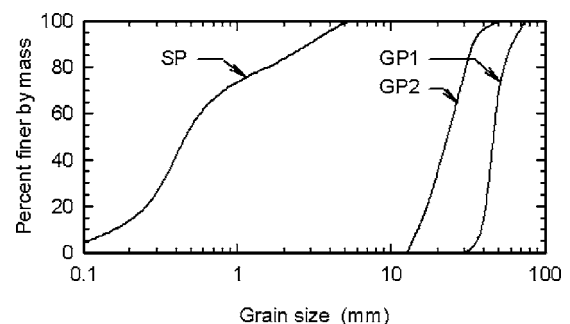


Fig. 2. Grain size distributions for poorly graded sand (SP) and poorly graded gravel (GP1 and GP2)

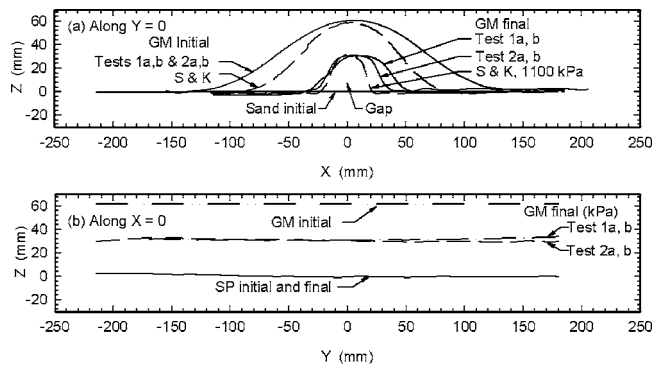


Fig. 3. Initial and deformed wrinkle shapes with sand above and below geomembrane: S&K=Soong and Koerner (1998): (a) along $Y=0$; (b) along $X=0$

because they were essentially identical. The deformed wrinkle shape is very similar to that of Test 1, despite the difference in applied pressure. A pressure of 1,100 kPa resulted in only 1 mm additional decrease in height as compared to 250 kPa. The wrinkle becomes narrower, experiencing 10 mm more reduction in width as the pressure increases from 250 to 1,100 kPa. Because the deformations of the geomembrane are largely controlled by soil deflections and the majority of wrinkle deflection takes place at lower pressures (Brachman and Gudina 2002), larger stresses will mainly influence the lateral deflection of the geomembrane, thus making the wrinkle narrower. Narrower wrinkles have a higher curvature, especially around the crest ($X=0$). Because curvature is related to strain, there is a greater likelihood of the geomembrane sustaining larger strains under larger overburden pressures. Similar to Test 1, there was little variation in wrinkle deflection along the Y -axis [Fig. 3(b)] for Test 2. The coefficient of variation was less than 4%. There is no discernible influence from the end boundaries, even at a pressure of 1,100 kPa.

Tests 2a and b were conducted with similar materials to those used by Soong and Koerner (1998), with the same initial wrinkle height but with a slightly larger initial width. Other differences were that their tests were conducted in a smaller ($0.3 \text{ m} \times 0.3 \text{ m}$) apparatus with no mention of friction treatment, and applied pressures were sustained for a longer test duration (1,000 h). Their results are also shown in Fig. 3(a) and are very similar to Tests 2a and b. The differences in reduction of wrinkle height and width between Soong and Koerner (1998) and Test 2 were only 5 and 4%, respectively. These differences are believed to arise principally from differences in testing boundary conditions (e.g., apparatus size and extent of boundary friction), although multiple differences between the tests prevent any firm conclusions.

Fate of Gap Beneath Geomembrane Wrinkle

Similar to the observations of Soong and Koerner (1998), the results in Fig. 3 all show that, with sand above and below the geomembrane, the gap beneath the wrinkle reduces in size but remains, even when subjected to applied pressures as large as 1,100 kPa. It was only in a test conducted to very large pressures of 3,000 kPa (Brachman and Gudina 2002) that the gap was eliminated because of deformation of sand into the region beneath the wrinkle.

When tested with clay below the geomembrane, the gap may be eliminated, depending on the applied pressure and clay sub-

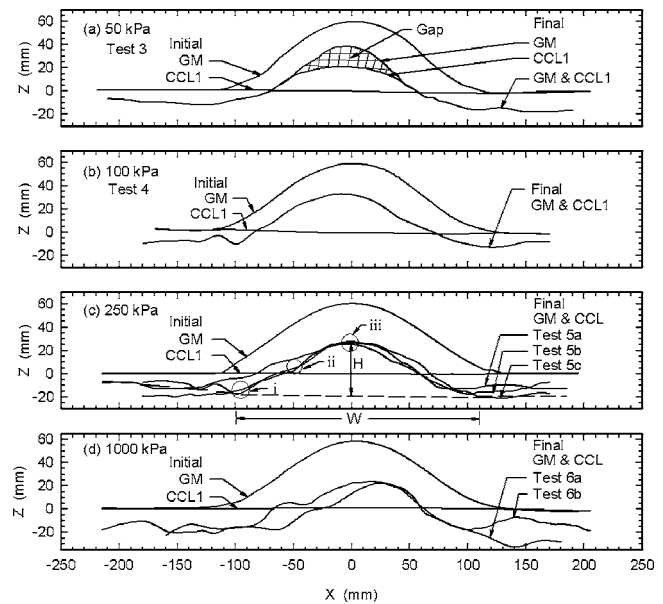


Fig. 4. Initial and deformed wrinkle shapes with subgrade CCL1, backfill GP1, and no protection at applied pressures of: (a) 50 kPa; (b) 100 kPa; (c) 250 kPa; and (d) 1,000 kPa

grade stiffness and strength. The influence of pressure on the fate of the gap with subgrade CCL1 (Tests 3–6) is plotted in Fig. 4. For Test 3 conducted to 50 kPa, an 18-mm-high and 90-mm-wide gap remained between the geomembrane and clay [Fig. 4(a)]. At 50 kPa on either side of the wrinkle ($|x| > 100 \text{ mm}$), there was downward vertical deflection of the geomembrane and clay associated with deformation of the underlying clay. Beneath the wrinkle ($|x| < 70 \text{ mm}$), the geomembrane moved downward while the clay surface moved upward. Because the clay was vertically unconfined beneath the wrinkle and the clay was compressed adjacent to the wrinkle, the clay beneath the wrinkle was subjected to a net upward displacement, resulting from extrusion of clay towards the unconfined region. The downward movement of the geomembrane and upward displacement of clay were such that the gap remained at 50 kPa.

The gap was completely eliminated at applied pressures of 100 kPa and larger, as indicated in Figs. 4(b–d), which shows that the final geomembrane and CCL1 surfaces were identical. Contact between the geomembrane and clay was confirmed by the transfer of ink marks drawn on the underside of the geomembrane to the clay surface beneath the wrinkle. At pressures of 100 kPa and larger, the upward movement of the clay relative to the downward movement of the wrinkle was such that the gap beneath the wrinkle was eliminated.

For all tests conducted with CCL1, the gap was eliminated at a pressure of 250 kPa regardless of the gravel backfill (GP1 and GP2) or protection layer (none, GT1, GT2, and SP) tested. These tests were conducted with relatively rapid increments in applied pressure (50 kPa every 10 min) such that the clay response was largely undrained. To assess whether the adopted loading rate influenced the observation that the gap was eliminated after a certain pressure, Test 7 was conducted by applying the pressure in smaller increments for a 12 h period, allowing the clay to exceed 90% consolidation for each increment. Other than the loading rate, Test 7 was identical to Test 5. The results for Test 7 are not plotted in Fig. 4(c) but were within the range of results obtained from the three duplicate Tests 5a, b, and c. This indicates that, for

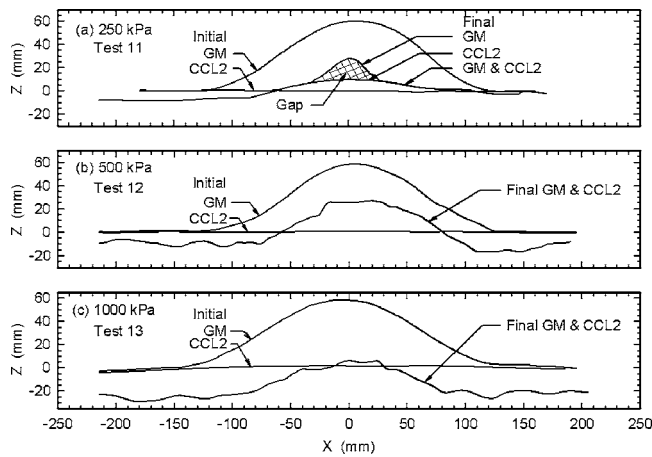


Fig. 5. Initial and deformed wrinkle shapes with subgrade CCL2, backfill GP1, and GT2 protection at applied pressures of: (a) 250 kPa; (b) 500 kPa; and (c) 1,000 kPa

the conditions examined, the gap was eliminated regardless of whether the clay was tested in a drained or undrained manner.

The results in Fig. 4 were obtained for clay placed and compacted at a water content of 16%, corresponding to a water content equal to $\omega_{opt} + 4\%$, which is the likely upper limit on molding water content for a clay liner (Benson et al. 1999). The same clay would be stiffer and stronger if compacted at a water content closer to ω_{opt} , which would be the lower limit of acceptable water contents in the field. To investigate the influence of the clay stiffness on the fate of the gap, results from Tests 11–13 conducted with CCL2 at a molding water content of 13% (i.e., $\omega_{opt} + 1\%$) are presented in Fig. 5. At 250 kPa [Fig. 5(a)], the stiffer and stronger CCL2 resulted in less clay compression away from the wrinkle and less clay heave beneath the wrinkle, both relative to CCL1. Consequently, the gap between the geomembrane wrinkle and the clay was reduced, but not eliminated at 250 kPa. For pressures of 500 kPa and greater, the gap was eliminated with CCL2 [Figs. 5(b and c)]. Therefore, the stiffness of the clay subgrade can have a significant influence on the fate of the gap beneath the wrinkle, with stiffer clay requiring a larger pressure for the gap to be eliminated.

An interesting observation of cracking of the clay surface beneath the wrinkle was seen for all tests with compacted clay, regardless of whether or not the gap beneath the wrinkle was eliminated. The extent of observed cracking is shown in Fig. 6, which was from Test 5b, but it is typical for all other tests conducted. This cracking is attributed to tensile strains in the clay beneath the wrinkle. For lower pressures, only hairline cracks were observed, while for pressures of 1,000 kPa, the cracks were about 3 mm wide and 5 mm deep. The cracks were up to 100 mm long and were observed along the wrinkle crest. The majority of

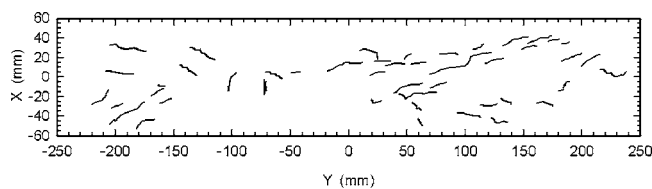


Fig. 6. Typical pattern of observed cracks on clay surface beneath wrinkle

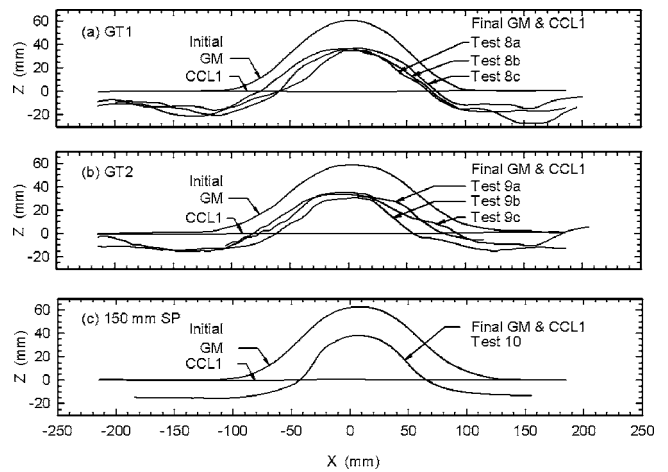


Fig. 7. Initial and deformed wrinkle shapes with subgrade CCL1, backfill GP1, and applied pressures of 250 kPa with protection layers of: (a) nonwoven needle-punched geotextile GT1 (390 g/m²); (b) nonwoven needle-punched geotextile GT2 (1,200 g/m²); and (c) 150-mm-thick sand SP

the cracks observed were not interconnected. The extent to which these cracks alter the transmissivity of the interface between the geomembrane and clay remains to be determined. It is possible that reductions in transmissivity expected from the improved contact between the geomembrane and CCL may not be fully realized due to increases in transmissivity from tensile cracking.

Wrinkle Deformations When Overlying Compacted Clay

Deformations of the geomembrane wrinkle when overlying compacted clay are also of interest. In addition to the deformed shapes plotted in Figs. 4 and 5, results obtained with differing protection layers are presented in Fig. 7 and with the 25 mm gravel backfill in Fig. 8. The final wrinkle height (H) and width (W) of the wrinkle as well as the maximum curvature (κ) in the vicinity of the wrinkle crest ($X \leq |50|$ mm) for all tests are summarized in Table 1. Final values of H and W were obtained relative to the deformed GM and CCL surfaces adjacent to the wrinkle, as illustrated in Fig. 4(c). Curvature was calculated by first approximating the deformed shape of the geomembrane with a higher order polynomial $f(X)$. Then, using first- [$f'(X)$] and second-order [$f''(X)$] central difference approximations, the curvature was calculated every 0.1 mm along the wrinkle using (Kreyszig 1999)

$$\kappa = \frac{|f''(X)|}{[1 + (f'(X))^2]^{3/2}} \quad (1)$$

Of all the factors tested, the subgrade beneath the wrinkle had the greatest effect on the wrinkle deformations. These differences

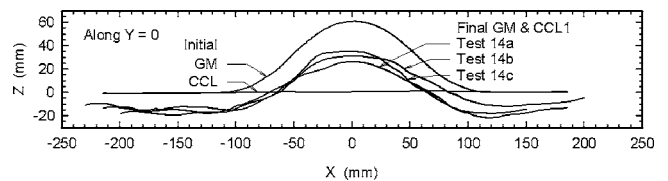


Fig. 8. Initial and deformed wrinkle shapes with subgrade CCL1, backfill GP2, and GT2 protection at applied pressures of 250 kPa

Table 3. Measured Local Indentations and Calculated Strains in Geomembrane

Test	Protection	Maximum indentation (mm)			Calculated strain at maximum indentation (%)		
		Beside wrinkle	Along wrinkle	Wrinkle crest	Beside wrinkle	Along wrinkle	Wrinkle crest
5a	None	11	4	2	42	25	5
8b	GT1	6	3	1	14	15	4
9b	GT2	3	2	1	11	10	1
10	150 mm SP	1	<1	<1	2	<1	<1

are most pronounced with CCL1 as the subgrade relative to SP. For example, comparing the results from Test 5 [Fig. 4(c)] with those from Test 1 [Fig. 3(a)] shows that the clay beneath the geomembrane results in a slightly higher and much wider wrinkle than with the sand subgrade. The extrusion of clay into the gap beneath the wrinkle is believed to resist further decreases in height and width of the wrinkle. This has a greater effect on the final width than the height. The much narrower wrinkle with the sand subgrade results in maximum wrinkle curvatures that are twice as large as those with the clay subgrade from Test 5 (see Table 1). Although there is a difference in the backfill used for Tests 1 and 5 (SP versus GP1 backfill), the difference in geomembrane deformations is largely attributed to the difference in subgrade (i.e., sand versus clay) rather than the overlying backfill. This hypothesis is supported by the results of Test 10, which had similar subgrade conditions and results to Test 5, but similar overlying sand to Test 1. Although having coarse gravel above the geomembrane does not appear to significantly alter the wrinkle deformations relative to sand backfill, the principal effect of the coarse gravel is to induce local deformations (and thereby strains) in the geomembrane, as discussed later.

Of all the tests conducted with gravel backfill, the largest difference in wrinkle deformations occurred between using CCL1 and CCL2 as the subgrade. For example, the results in Fig. 5(a) with the stiffer CCL2 (Test 11) show a shorter and narrower wrinkle than those in Fig. 7(b) with CCL1 (Test 9), but with otherwise identical test parameters. The smaller subgrade deformations with the stiffer CCL2 permitted the wrinkle to experience greater deformations than with CCL1. Also, because the gap beneath the wrinkle was not completely filled with clay in Test 11, the wrinkle was able to experience a greater decrease in width than for Test 9. The deformations are such that the maximum curvature from Test 11 is greater than three times larger than the average value from Test 9 (see Table 1).

Similar to the results with sand, increasing the applied pressure with a clay subgrade initially produced decreases in wrinkle height and width and then had little additional effect at higher pressures. For example, as shown in Fig. 4 with CCL1, increasing the pressure to 100 kPa reduces the wrinkle height and width to 40 and 190 mm, respectively. Once the gap beneath the wrinkle is eliminated (100 kPa and larger), further increases in pressure result in no further decrease in wrinkle size. Also, the final curvature is not greatly affected by pressure with CCL1, increasing from 2.5×10^{-2} at 250 kPa [Test 5(c)] to a maximum value of 3.2×10^{-2} in Test 6a at 1,000 kPa. However with the stiffer clay CCL2, a much larger curvature was measured at 1,000 kPa (Test 13) than at lower pressures (Tests 11 and 12), as summarized in Table 1. The large curvature of 21×10^{-2} for Test 13 was not caused by changes in height and width of the wrinkle, but rather from local pinching of the geomembrane [induced at $X=26$ mm in Fig. 5(c)] from the overlying coarse gravel.

The type of protection layer did not have a significant influ-

ence on wrinkle deformations when subject to 250 kPa of vertical pressure. For example, the deformed shape with either GT1, GT2, or 150 mm SP as the protection layer, plotted in Figs. 7(a–c), respectively, are similar to those obtained with no protection and otherwise identical test parameters [Test 5, Fig. 4(c)]. As summarized in Table 1, the curvature at 250 kPa increased slightly with inclusion of a protection layer, with maximum values of 3.3, 3.0, and 3.2×10^{-2} for tests with GT1, GT2, and SP (Tests 8a, 9b, and 10, respectively), as compared to 2.5×10^{-2} without protection (Test 5c).

Fig. 8 shows that the 25 mm gravel GP2 (Test 14) produced essentially the same final wrinkle geometry as with GP1 (Test 9), for otherwise the same test conditions. Likewise, a smaller initial wrinkle height of 30 mm (see Test 15 in Table 1) did not play a major role in the wrinkle deformations, because a similar decrease in height and width as a proportion of their original values was measured relative to those with $H_0=60$ mm.

Effect of Wrinkle, Protection Layer, and Gravel on Local Geomembrane Indentations

Local indentations in the geomembrane may develop from the overlying coarse gravel. The protection layer is intended to prevent puncture and limit the long-term tensile strains of the geomembrane at these indentations. While the geomembrane was not punctured in any of the short-term tests conducted, the magnitude of the local indentations (and hence the geomembrane strain) was affected by the presence of the wrinkle, the type of backfill, and the type of protection layer. Geomembrane strains were calculated from measured indentations using the procedure of Tognon et al. (2000) at three different locations: (1) beside the wrinkle; (2) along the wrinkle; and (3) at the crest of the wrinkle, as indicated in Fig. 4(c). Measured maximum indentations and calculated strains are reported in Table 3 for the tests with GP1, CCL1, and an applied pressure of 250 kPa.

The results in Table 3 show that the indentations were largest beside the wrinkle and smallest at the wrinkle crest. For example, with no protection layer, the maximum strain beside the wrinkle was approximately eight times larger than that at the wrinkle crest. Local indentations in the geomembrane are made even worse by the presence of the wrinkle. For example, the maximum strain without a wrinkle (from tests that are not reported in this paper but were identical to Test 5a other than with the geomembrane initially flat) was 32%, as compared to the maximum value of 42% with a wrinkle. Redistribution of stresses from above the wrinkle to either side from wrinkle deformations leads to higher contact forces beside the wrinkle and, consequently, results in larger local strains in the geomembrane.

While the protection layer did not significantly alter the deformed shape of the wrinkle, the results in Table 3 demonstrate that it was able to reduce the local geomembrane indentations. This can also be observed from the fact that the final wrinkle

becomes successively smoother as the protection layer varies from none in Fig. 4(c) to GT1, GT2, and SP in Fig. 7. Inclusion of GT1 reduced the maximum strain to one-third of that without protection, and the thicker GT2 resulted in even further decreases in maximum strain. The geomembrane beneath the 150-mm-thick sand protection layer was very smooth, with a maximum indentation anywhere around the wrinkle of approximately 1 mm. A maximum strain of 2% was calculated for a location away from the wrinkle, while there was no significant local indentation near the shoulder and crest of the wrinkle.

Of the protection layers tested at 250 kPa, only the 150-mm-thick sand layer had maximum strains below the 6% allowable strain criterion (for smooth materials with a stress crack resistance less than 1,500 h) of Peggs et al. (2005), while none were below the 0.25% allowable strain from indentations criterion of BAM (1995). While there is still debate on the maximum allowable strain for a geomembrane and the role that stress relaxation may play, it is clear that the wrinkle can increase the strains in the geomembrane.

Conclusions

Results from short-term physical experiments involving a wrinkle in a 1.5-mm-thick HDPE geomembrane were reported. The influences of subgrade, protection layer, backfill, and applied pressure on the fate of the gap beneath the wrinkle, the wrinkle deformations, and the local geomembrane indentations were examined, and the principal conclusions are as follows:

1. Fate of the gap beneath the geomembrane wrinkle: The gap was reduced but remained with sand above and below the geomembrane (up to 1,100 kPa). With compacted clay subgrade, the gap was completely filled with clay, depending on the applied pressure and the clay water content. The elimination of the gap was caused by downward vertical deformation of the geomembrane and upward vertical deformation of the clay. For the particular clay tested at water contents of 16% (CCL1) and 13% (CCL2), the gap was eliminated at pressures of 100 and 500 kPa, respectively.
2. Wrinkle deformations: Of the factors investigated, the wrinkle deformations were most influenced by the subgrade. The deformed wrinkle was slightly shorter, much narrower, and had a maximum curvature twice as large with sand subgrade as with clay. Clay water content influenced wrinkle deformations, as the stiffer CCL2 resulted in a shorter and narrower wrinkle with a maximum curvature three times larger than with CCL1. Increasing the applied pressure initially produced decreases in wrinkle height and width but then had little additional effect at higher pressures. The protection layers, backfill materials, and initial wrinkle geometries tested did not have a large influence on wrinkle deformations.
3. Local geomembrane indentations: Although the geomembrane was not punctured in any of the short-term tests conducted, it was subject to local indentations (and strains) from the overlying coarse gravel. For the specific conditions tested (applied pressure of 250 kPa, 50 mm gravel backfill, and CCL1 subgrade), the maximum short-term tensile strain in the geomembrane was 42% without protection, 15% with nonwoven needle-punched geotextile GT1 (390 g/m²), 11% with nonwoven needle-punched geotextile GT2 (1200 g/m²), and 2% with the 150-mm-thick sand protection layer. The maximum local strain beside the wrinkle was

found to be greater than that without a wrinkle in the geomembrane.

These results are applicable for the specific materials (backfill, protection layer, geomembrane, and subgrade) and conditions tested, and as such they should not be directly used for design purposes for different conditions. The reported deformations and strains are expected to underestimate those expected at the base of a landfill, because they were obtained from short-term tests conducted at 22°C and without chemical exposure. Work is currently underway to quantify the combined effects of applied stress, elevated temperature, and chemical exposure on geomembrane deformations.

Acknowledgments

Funding was provided by the Natural Sciences and Engineering Research Council of Canada, the Canadian Foundation for Innovation, and the Ontario Innovation Trust. The geomembrane was provided by Layfield Plastics and the geotextile protection layers by Naue Fasertechnik.

Notation

The following symbols are used in this paper:

- $f'(X)$ = first-order central difference approximation;
- $f''(X)$ = second-order central difference approximation;
- H = wrinkle height;
- H_0 = initial wrinkle height;
- W = wrinkle width;
- W_0 = initial wrinkle width;
- X = direction transverse to wrinkle;
- Y = direction along wrinkle axis;
- Z = vertical direction;
- κ = curvature;
- ω_{CCL} = water content of compacted clay; and
- ω_{opt} = Proctor optimum water content.

References

- ASTM. (1992). "Standard practice for determination of 2% secant modulus for polyethylene geomembranes." *ASTM D 5323*, West Conshohocken, Pa., 133–135.
- ASTM. (2001). "Standard test method for determining tensile properties of nonreinforced polyethylene and nonreinforced flexible polypropylene geomembranes." *ASTM D 6693*, West Conshohocken, Pa., 392–395.
- Bundesanstalt für Materialforschung und Prüfung [Federal Institute for Materials Research and Testing] (BAM). (1995). Anforderungen an die Schutzschicht für die Dichtungsbahnen in der Kombinationsdichtung: Zulassungsrichtlinie für Schutzschichten, Berlin (in German).
- Benson, C. H., Daniel, D. E., and Boutwell, G. P. (1999). "Field performance of compacted clay liners." *J. Geotech. Geoenviron. Eng.*, 125(5), 390–403.
- Brachman, R. W. I., and Gudina, S. (2002). "A new laboratory apparatus for testing geomembranes under large earth pressures." *Proc., 55th Canadian Geotechnical Conf.*, Canadian Geotechnical Society, Alliston, Canada, 993–1000.
- Geosynthetic Institute. (2003). "GRI test method GM13: Standard specification for 'test properties, testing frequency, and recommended warrant for high density polyethylene (HDPE) smooth and textured geomembranes'." *GRI-GM13*, Folsom, Pa.

- Kreyszig, E. (1999). *Advanced engineering mathematics*, 8th Ed., Wiley, New York.
- Ontario Ministry of the Environment (MoE). (1998). "Landfill standards: A guideline on the regulatory and approval requirements for new or expanding landfilling sites." *Ontario Regulations 232/98*. Queen's Printer for Ontario, Toronto.
- Peggs, I. D., Schmucker, B., and Carey, P. (2005). "Assessment of maximum allowable strains in polyethylene and polypropylene geomembranes." *Proc., Geo-Frontiers 2005* (CD-ROM), ASCE, Reston, Va.
- Pelte, T., Pierson, P., and Gourc, J. P. (1994). "Thermal analysis of geomembrane exposed to solar radiation." *Geosynthet. Int.*, 1(1), 21–44.
- Rowe, R. K., Quigley, R. M., Brachman, R. W. I., and Booker, J. R. (2004). *Barrier systems for waste disposal facilities*, E&FN Spon, London.
- Soong, T.-Y., and Koerner, R. M. (1998). "Laboratory study of high density polyethylene waves." *Proc., 6th Int. Conf. on Industrial Fabrics Association International, Geosynthetics*, St. Paul, Minn., 301–306.
- Tognon, A. R., Rowe, R. K., and Brachman, R. W. I. (1999). "Evaluation of side wall friction for a buried pipe testing facility." *Geotext. Geomembr.*, 17, 193–212.
- Tognon, A. R., Rowe, R. K., and Moore, I. D. (2000). "Geomembrane strain observed in large-scale testing of protection layers." *J. Geotech. Geoenviron. Eng.*, 126(12), 1194–1208.